Crystallization in Lactose Refining—A Review

Shin Yee Wong and Richard W. Hartel

Abstract: In the dairy industry, crystallization is an important separation process used in the refining of lactose from whey solutions. In the refining operation, lactose crystals are separated from the whey solution through nucleation, growth, and/or aggregation. The rate of crystallization is determined by the combined effect of crystallizer design, processing parameters, and impurities on the kinetics of the process. This review summarizes studies on lactose crystallization, including the mechanism, theory of crystallization, and the impact of various factors affecting the crystallization kinetics. In addition, an overview of the industrial crystallization operation highlights the problems faced by the lactose manufacturer. The approaches that are beneficial to the lactose manufacturer for process optimization or improvement are summarized in this review. Over the years, much knowledge has been acquired through extensive research. However, the industrial crystallization process is still far from optimized. Therefore, future effort should focus on transferring the new knowledge and technology to the dairy industry.

Keywords: crystallization, industrial, lactose, optimization, secondary nucleation

Introduction

The first record of the isolation of lactose was in 1633, by Bartolettus, through the evaporation of whey (Nickerson 1974). Ettmüller in 1688, improved Bartolettus' process of evaporation and included the purification of crude lactose by recrystallization (Whittier 1944). After that, the research activity in lactose production was very active in the 1900s. A better understanding of lactose crystallization was established and innovative production methods were reported.

Lactose has no flavor and low sweetness (30% of sucrose). Therefore, it is widely use to reduce the overall sweetness of confectionery or other products. In the food and confectionery industries, lactose is commonly used as a filler or flavor carrier (McSweeney and Fox 2009). In addition, lactose is a reducing sugar that enhances color and flavor generation in many bakery or confectionery products via Maillard and Strecker reactions (Boutin 2005). Nutritionally, it promotes the assimilation of calcium, and has been used in numerous nutritional products (Holsinger 1988). The principle application of lactose is in the preparation of infant formula. Lactose is added to cow's milk (≈ 5% lactose) to boost the lactose content to a level similar to human milk (≈ 7% lactose; McSweeney and Fox 2009). The purest form of α-lactose has been used by the pharmaceutical industry. In the manufacture of pharmaceutical tablets and capsules, lactose is widely used as an excipient (filler or filler-binder; Booij 1985), a carrier for inhalation aerosols (Zeng and others 2000), or dry powder inhalers (DPI; Kirk and others 2007).

In the dairy industries, lactose is produced from whey or whey permeate which are by products from the production of cheese and/or caseinates. Recovery (Ganzle and others 2008) of lactose from whey enhances both the improvement of the economics of whey utilization and the pollution reduction as lactose recovery can reduce the biochemical oxygen demand of whey by more than 80% (Bund and Pandit 2007). However, in the food industry, the current lactose manufacturing process is still far from optimized. The majority of industrial lactose crystallization process produces a large population of small crystals, which limits the separation efficiency of the downstream processes, resulting in low recovery. Part of the reason for this might be because of the lack of understanding of crystallization process behavior under dynamic conditions. Therefore, the objective of this review is to highlight some of the important theories and studies of lactose crystallization.

MS 20130424 Submitted 3/26/2013, Accepted 12/2/2013. *Author Wong is with Dept. of Biological Systems Engineering, Univ. of Wisconsin, Madison, WI, 53706. Author Hartel is with Dept. of Food Science, Univ. of Wisconsin, Madison, WI, 53706. Direct inquiries to author Hartel (E-mail: rwhartel@wisc.edu).*

Characteristics of Lactose

Properties and crystal shapes

Lactose is a disaccharide composed of galactose and glucose connected by a $\beta(1\rightarrow4)$ glycosidic bond (McSweeney and Fox 2009). Because of the presence of a chiral carbon, lactose can exist in 2 forms (isomers): α or β lactose. Lactose is most frequently found as hydrated α-lactose monohydrate crystal. The other polymorph, anhydrous β-lactose, is less common and it crystallizes above 93.5 °C. The α and β anomers have very different properties. The polymorphs can be distinguished by the specific rotation (+89° and +35° for α- and β-lactose, respectively) and solubility (70 and 500g/L (at 20 °C) for α- and β-lactose, respectively (McSweeney and Fox 2009).

A schematic diagram of a typical α-lactose monohydrate crystal is shown in Figure 1. The α-lactose crystals are monoclinic sphenoidal and have only 1 axis of symmetry. They have trapezoidal side faces, rhombic tops and bottoms, and beveled faces at the base and apex, giving the crystal a distinct tomahawk appearance (Hunziker and Nissen 1927). Microscopic images of both α- and β-lactose crystals are shown in Figure 2. They can exist in a wide variety of shapes, depending on the types and conditions of crystallization (Nickerson 1974). For slow crystallization from solution, α-lactose monohydrate has a characteristic tomahawk-like shape (Figure 1), whereas crystals of β-lactose have an uneven-sided diamond shape (Listiohadi and others 2005).

Solubility and mutarotation

Lactose molecule has a hemiacetal structure. The ring structure (opening or forming) enables the molecule to interchange between α and β anomers, that is, a process known as mutarotation (McSweeney and Fox 2009). In aqueous solutions, the α and β

doi: 10.1111/1750-3841.12349

equilibrium depend on the temperature, concentration, pH, and presence of foreign substances in the solution (Hartel and Shastry 1991). For example, at 20 °C, the optical rotation will change (because of the mutarotation process of α form into the β form or vice versa) until a specific rotation of +55.3° is reached at the equilibrium, regardless of the form used to prepare the starting solution (Ganzle and others 2008). This is about 1.5 parts of β-lactose for every part of α-lactose in solution (Hunziker and Nissen 1926).

When α-lactose monohydrate crystals are added to water in excess over the saturation concentration, initial concentration is first achieved by rapid dissolution of a portion of the crystals (expressed as initial solubility by Hunziker and Nissen, 1926). Below the solubility limit, the rate of α-lactose monohydrate crystals dissolving into water is limited by the surface reaction of disassociation of α-lactose molecules from the crystal structure (Lowe and Paterson 1998). However, after a α-lactose molecule is in solution, mutarotation (transformation of α to β form) takes place, and the final solubility (equilibrium of α and β forms) is achieved as more of the α-lactose monohydrate crystals dissolve (Hunziker and Nissen 1926). Total lactose solubility versus temperature is shown in Figure 3.

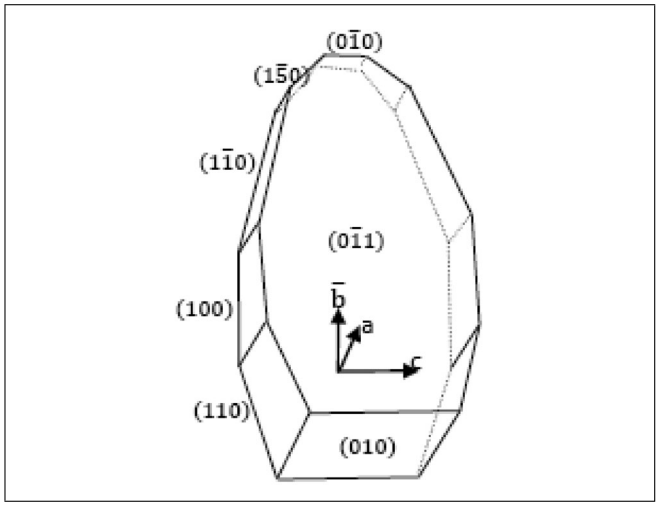

Figure 1–Tomahawk crystal of α-lactose monohydrate showing faceted structure.

Table 1–Composition of whey permeate and concentrate.

Component	Whey permeate (%; Wood-Kaczmar 2006)	Whey permeate concentrate (%) (industrial source)
Protein	0	Trace
Lactose	4.8	≈ 39 to 56
Ash	0.8	≈ 5 to 7
Non protein nitrogen	0.18	≈ 1 to 2
Fat	0	Trace
Total dry matter	5.78	≈ 65 to 70

The choice of solvent and presence of salts or sucrose influences both the mutarotation and the solubility of lactose (Harper 1992). For example, Majd and Nickerson (1976) reported that the solubility of lactose in aqueous mixtures with alcohol is inversely proportional to the alcohol concentration, and alcohol chain length.

In lactose refining, lactose crystals are obtained from whey or whey permeate, which contain traces of whey protein and minerals. Typical compositions of whey permeate and concentrate are shown in Table 1. In Figure 3, the solubility of lactose in whey permeate systems are compared against the solubility of lactose in water. Similar to other reports (Ganzle and others 2008), the lactose solubility varies in different whey permeate systems. Lactose is consistently a little less soluble in whey permeate systems, depending on mineral concentration and composition. The reduced solubility of lactose in whey may be because of alteration in bulk water structure because of the presence of impurities (Bhargava and Jelen 1996). In the whey permeate system, some ions of low charge density (Cl^-, Br^-, I^-) may cause perturbation and water structure breaking, whereas others of high charge density (Li^+, Ca^{2+}, Ba^{2+}, Sr^{2+}) may orient the water structure.

Mechanisms of lactose crystallization

Crystallization is generally considered as a 2-step process involving (1) nucleation and (2) growth of the nucleus. The process of the initial creation of zero-sized crystals (nuclei) is called nucleation. The nuclei will grow depending on the available supersaturation.

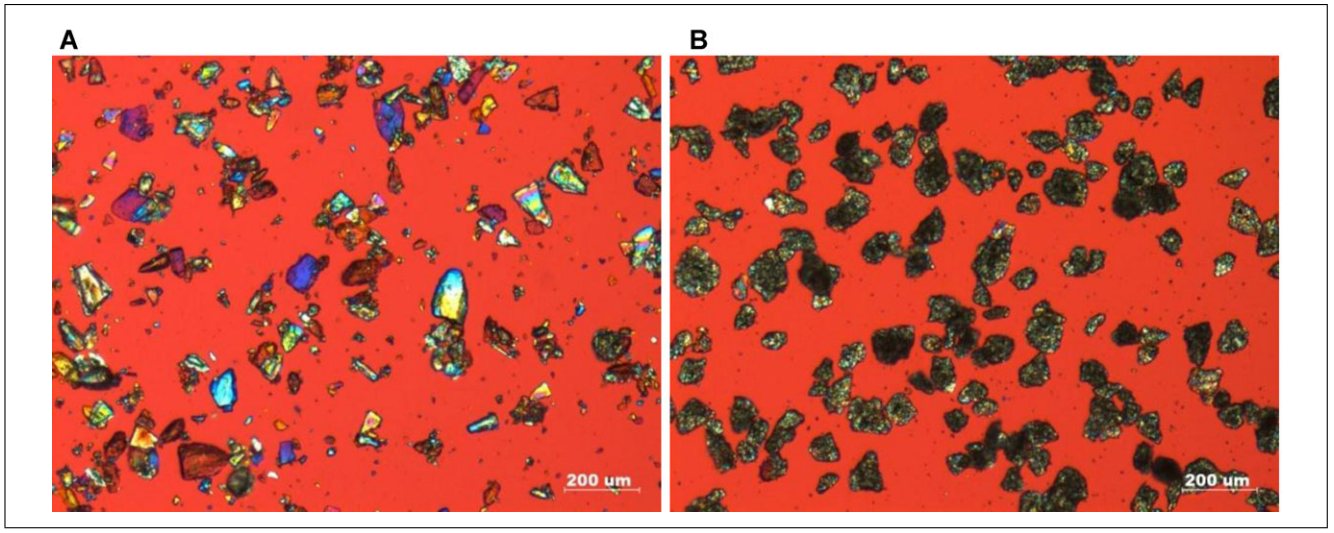

Figure 2–Polarized light microscopic images of (A) α-lactose monohydrate (Pharmaceutical grade lactose 310, Foremost Farm, Baraboo, Wis., USA) and (B) anhydrous β-lactose crystals (β -D-Lactose, Acros Organics, Fair Lawn, N.J., USA).

In addition, particle disruption can occur through secondary nucleation, aggregation or breakage.

Supersaturation (S), the driving force of crystallization, can be defined in thermodynamic terms as the dimensionless difference in chemical potential between a molecule in an equilibrium state and a molecule in its supersaturated state (Davey and Garside 2000). However, chemical potential cannot be easily determined. Therefore, S is expressed as solution concentration. Visser (1982) developed a model (Eq. 1) for supersaturation of α-lactose solution in mutarotation equilibrium below 93.5 °C,

$$S = \frac{C}{C_s - F K_m (C - C_s)} \quad (1)$$

$$C_s = 12.23 + 0.3375T + 0.001236T^2 + 0.00007257T^3 + 5.188\text{x}10^{-7}T^4 \quad (2)$$

$$F = \exp\left(\frac{-2374.6}{T_k} + 4.5683\right) \quad (3)$$

$$K_m = -0.002286T + 2.6371 \quad (4)$$

Here, C is the total lactose concentration of the solution (g anhydrous lactose/100 g water), C_s is the final solubility of lactose (g anhydrous lactose/100 g water), F is a temperature-dependent factor for depression of solubility of α-lactose by β-lactose, K_m is the ratio of β/α lactose in mutarotation equilibrium, T is the temperature in °C, and T_k is the temperature in K.

Nucleation

Nucleation occurs because of clustering and aggregation of molecules or ions in a solution, vapor or supersaturated melt. Upon nucleation, these clusters are stable and grow to a detectable size. As shown in Figure 4, nucleation can be categorized into primary and secondary nucleation. Primary nucleation occurs either in the presence (heterogeneous) or absence (homogeneous) of suspended particles that catalyze formation of stable clusters. Nucleation by strict homogeneous nucleation is unlikely during lactose refining because of the presence of impurities that act as heterogeneous nucleation sites (Hartel and Shastry 1991). In addition, lactose refining operates at relatively low supersaturation where homogeneous nucleation does not occur. At lower supersaturations and temperatures, the energy available in the supersaturated solution is insufficient to cause nuclei formation by homogenous nucleation (Shi and others 1989; Mcleod 2007). Therefore, heterogeneous nucleation is the main source of initial nuclei generation. After that, secondary nucleation dominates.

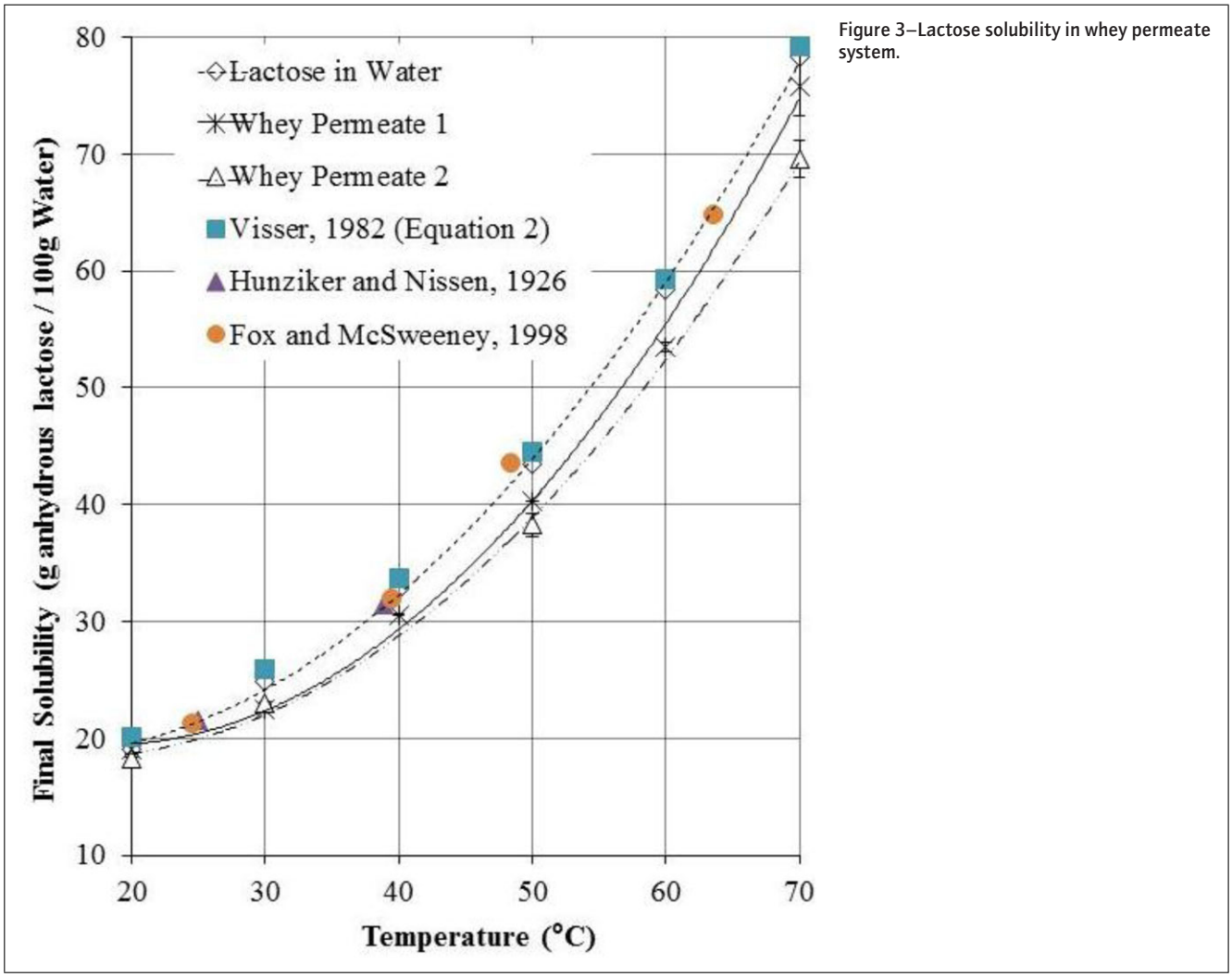

Figure 3–Lactose solubility in whey permeate system.

Secondary nucleation occurs only when existing seed crystals (or something of the same form) are present in the system. Compared to primary nucleation, secondary nucleation has lower activation energy, and can be triggered at low levels of supersaturation (1.6× the solubility limit; Mcleod 2007). For industrial lactose refining, secondary nucleation of the type of induced/contact nucleation is common (Shi and others 1989; Jones 2002; Shi and others 2006). In an industrial stirred crystallizer, contact nucleation can be triggered by suspended crystals–crystals, crystals—impeller, or crystals–vessel walls collisions. After the collision, potential sources of nuclei includes (1) parts of crystals breaking off from the contact surfaces; (2) embryos of sufficient size originated from the hypothetical growth layer surrounding the seed crystals; which are then released into the solution (Shi and others 1989).

Induction time is often used to characterize the rate of nucleation. Induction time is defined as the time elapsed between the initiation of supersaturation to the formation of nuclei. At a fixed temperature, induction time is generally considered to be inversely proportional to the solution concentration. Herrington (1934a) studied the correlation of induction time and the degree of supercooling and supersaturation for nucleation. The value of the induction time can be categorized using the regions outlined in the lactose "supersolubility" diagram (Figure 5). In the labile zone, the induction time was circa 36 h when the lactose solution concentration was 1.1 to 1.3 times higher than the concentration at super-solubility line. The induction time was reduced to less than 10 h at higher concentration. Different values of induction times were reported in the metastable region, separated by the forced crystallization lines. The values reported were 360 h and 136 h in the upper and lower metastable zone, respectively. In the undersaturated region, the solutions are stable to crystallization and no significant nucleation was reported even after 360 h.

The impacts of some processing parameters on the nucleation rate are summarized in Table 2. Most of the studies focused on secondary nucleation except the studies by McLeod and others (2010) and Raghavan and others (2001). From the table, it is clear that all processing parameters have an impact on the nucleation rate and they are highly interactive. Based on the experimental observations listed in Table 2, two different strategies aimed at controlling secondary nucleation in lactose refining have been proposed:

First, Shi and others (2006) studied lactose crystallization with different level of seed crystals, and reported that there exists an optimal number of nuclei (27 mg/100 g solution) for the generation of large, uniformly sized crystals (>500 μm) with very limited number of secondary nuclei developing into small crystals. They argued that secondary nuclei can be inhibited by balancing crystal growth and clusters to crystals conversions rates. Therefore, to avoid secondary nucleation, a suitable number of existing crystals, which were derived from an optimal number of initial nuclei by primary induced nucleation and that are in fast growing status, is necessary. After the generation of initial nuclei, the mode of crystal–crystal and crystal–crystallizer contacts (frequency, intensity, contact area, contact time) should be kept to a minimum to provide gradual transition to the crystal growth phase. With this approach, 500 μm crystals were grown in just 3 h.

In another batch crystallization study, Wong and others (2012) refined the lactose "supersolubility" diagram (Figure 5) according to the extent of secondary nucleation. A general strategy was recommended to control the crystallization operation in the upper metastable zone width (MSZW) with minimal agitation rate (just sufficient to maintain crystal suspension). The refined diagram and recommended process will be discussed further in the section on approaches to improve lactose refining.

Crystal growth

The mechanism of crystal growth generally consists of 3 successive steps: (1) mass transport (diffusive or convective) from the bulk to the crystal surface, (2) surface reaction/integration, and

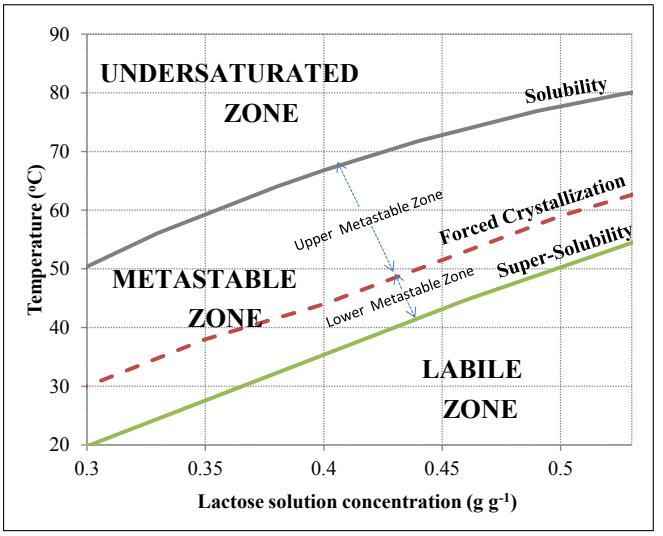

Figure 5–Lactose "supersolubility" diagram proposed in 1926.

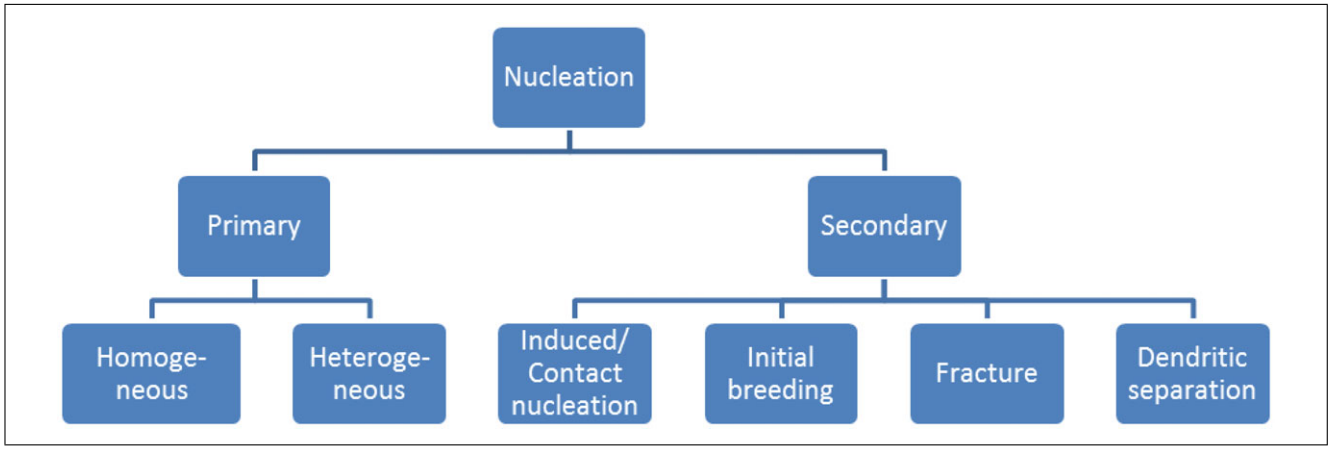

Figure 4–Categorization of nucleation mechanism.

Table 2–Summary of the impact of processing parameters on primary (PN) or secondary nucleation (SN) rates.

Process parameters	Mode	Impact	Reference
Mixing	PN	Greater flow instability leads to higher extent of nucleation events. However, once the instability reaches a critical value, the extent of nucleation flattens. Flow instability can be created by varying the level of cavitation, power input, Reynolds number, and vortex formation.	(McLeod and others 2010)
		Induction time reduces with agitation up to a certain speed beyond which it remains constant.	(Raghavan and others 2001; McLeod and others 2010)
β-lactose	PN	Large quantity of β-lactose in solution acts as a nucleation inhibitor.	(Raghavan and others 2001)
Supersaturation	SN	There exists a critical supersaturation for contact nucleation by sliding mechanism (boundary of forced nucleation)	(Shi and others 1989)
		At fixed temperature, nucleation rate increases with lactose solution concentration. There is gradual increase when the concentration is in a lower range but it becomes very sharp when the concentration is higher than 55% to 60%.	(Shi and others 2006)
Temperature	SN	Nucleation rate increases with temperature	(Shi and others 1990)
Seed crystals	SN	Existence of lactose seed is necessary to result in secondary nucleation or to reduce the induction time.	(Griffiths and others 1982; Shi and others 1989)
		Secondary nucleation can be controlled by a suitable number of initial nuclei (seed) that are in fast growing status.	(Shi and others 2006)

(3) transport of latent heat away from the growing crystals. For lactose crystallization, the growth rate is considered to be surface integration controlled (Kreveld and Michaels 1965; Nickerson and Moore 1974; Hartel and Shastry 1991).

The growth of lactose crystals is affected by some process parameters and solution characteristics, including supersaturation, temperature, viscosity, pH, and presence of impurities (Bhargava and Jelen 1996). Supersaturation is generally reported as the dominant parameter that determines the growth rate directly, whereas the other parameters have an indirect effect on supersaturation, the rate of mutarotation or heat, and mass transfer rate. The pH influences the rate of mutarotation, and thus is an important factor in lactose crystallization (Nickerson and Moore 1974; Ganzle and others 2008). Mutarotation is accelerated by alkali (pH > 7) and high acidic condition (pH < 1). However, organic acids normally found in whey, such as acetic and lactic acids, do not produce the low pH required and thus, act as inhibitors to lactose crystallization (Nickerson and Moore 1974). Ideally, lactose should be crystallized from sweet whey with as high a pH as practically possible (Modler and Lefkovitch 1986). However, highly alkaline conditions (pH > 10) may catalyze the formation of lactose degradation products that may inhibit crystallization (Nickerson and Moore 1974; Ganzle and others 2008).

The effects of some important process parameters on lactose crystal growth are summarized in Table 3, which shows that the effects of all processing parameters are highly interactive. Thus, in the literature, all optimal crystallization conditions are defined based upon the condition of other parameters. For example, in the refining process invented by Shi and others (2006), it was reported that the maximum growth rate occurred at 40 °C to 50 °C for a system with a relatively high supersaturation (at least 58% lactose) and an optimal numb**e**r of nuclei. Therefore, to control the growth rate, all parameters should be taken into account to achieve the desired product quality.

During the production of lactose, it is sometime necessary to control the morphology of the lactose crystal. For example, when used as an excipient for inhalation aerosols, the lactose morphology (size, shape, surface texture) is believed to have an impact on the delivery of the drug (Zeng and others 2000). Lactose crystals of different crystalline habit may be formed according to the relative growth rates of different faces (Figure 1), depending upon the conditions of crystallization (Hunziker and Nissen 1927; Herrington 1934b; Hartel and Shastry 1991; Garnier and others 2002). When the growth rate is high (for example, at high supersaturation), elongated crystals (Zeng and others 2000) or prisms (needles; Hartel and Shastry 1991; Zeng and others 2000) are formed. As the growth rate decreases (for example, at low supersaturation), the crystal will transition to tomahawk (Hartel and Shastry 1991; Zeng and others 2000) or diamond-shaped plates (Herrington 1934a).

In addition, the presence of additives also affects the crystalline habit. A list of additives and their impact on crystal growth and shape are summarized in Table 4. The influence of additives on crystal growth generally includes some or all of the following:

(1) Reduce solubility of lactose in the presence of additives, leading to higher degree of supersaturation and thus, an increase in the growth rate. For example, the major minerals present in whey influence the solubility of lactose in supernatant liquor during crystallization (Figure 3).
(2) Retard crystal growth by incorporation of the impurities/additives into the lactose crystal lattice and act as disrupting impurities (Clydesdale and others 1994). For example, the anionic form of lactose phosphate (LP) molecules are adsorbed at the lactose crystal faces ([010] and [110]) where their free glucose group can be integrated (Visser and Bennema 1983). Depending on the amount of LP present at the beginning of the crystallization process, the percentage of the LP that integrates into the final crystals was found to be between 60% and 80% of the initial amount (Lifran and others 2007).
(3) Affect the deposition of lactose on the surface of the lactose crystal (Nickerson and Moore 1974). Calcium and phosphate accelerate the growth rate in the absence of other minerals (Jelen and Coulter 1973a; Guu and Zall 1991). It is likely that the salt accelerates the surface deposition step of the crystallization process (a function of thermodynamic activity), in addition to lowering the lactose solubility (in whey) and accelerating the mutarotation reaction (Jelen and Coulter 1973a).
(4) Bind with water and create local lactose supersaturation spots that are favorable for nucleation, promoting the production of small crystals/nuclei and retarding crystal growth. For instance, whey protein binds with water, and results in the production of high number of small crystals, which is a result of high nucleation rate (Mimouni and others 2005).

Table 3–Summary of the impact of processing parameters on growth rate.

Process parameters	Impact	Reference
Supersaturation	Growth rate increases with supersaturation, but it decreases again as mobility decreases (viscosity increases) near glass transition temperature (T_g).	(Kreveld and Michaels 1965; Shi and others 1989; Garnier and others 2002; Mcleod 2007)
Temperature	The rate of mutarotation is higher at high temperature.	(Thurlby 1976; Shi and others 1989, 1990; Jelen and Coulter 1973b)
	The viscosity is lower at high temperature, which is beneficial for mass transfer and nucleation control.	(Shi and others 2006)
	An increase in temperature would accelerate the dissolution of crystal surface distortions, resulting in improved surface smoothness.	(Zeng and others 2000)
	At temperature below or near T_g the translational mobility of lactose is not possible and crystallization is kinetically limited.	(Roos 2009)
Cooling rate/profile	Slow cooling produces crystals that are uniform in size	(Valle-Vega and others 1977)
pH	Change mutarotation equilibrium and the growth rate of the different faces of α-lactose	(Nickerson and Moore 1974; Raghavan and others 2001; Ganzle and others 2008)
Hydrodynamics (agitation)	Temperature distribution, heat transfer	(Wood-Kaczmar 2006)
	Distribution of solids (crystals), convective mass transfer	(Mcleod 2007)
	Agitation rate is not important if all crystals are suspended	(Shi and others 2006)
	Strong agitation and mechanical impact triggers secondary nucleation	
Number of crystal present in the system	Increase growth rate dispersion when the number of crystal present in the system increases, resulting in wider variation in the growth rates of very small crystals.	(Randolph and Larson 1988)

Aggregation

Crystal aggregates are multiple crystals that fuse together into a single particle. They are usually formed when rapidly growing crystals contact each other. In particular, small crystals in the initial growth phase after nuclei generation or those with a large difference in crystal size are prone to form aggregates (Shi and others 2006). It is believed that the aggregation of crystals might occur through nucleus bridges between the crystals during bulk crystallization (Linnikov 2008). The Smoluchowski equation (for coagulation of colloidal particles) was modified by Linnikov (2008) to describe crystals aggregation:

$$-\frac{\mathrm{d}N}{N^2} = K_a \,\mathrm{d}\tau \tag{5}$$

$$K_a = \mathrm{K_o}\, P\, V^{-1}\, W W_1 \tag{6}$$

In these equations, aggregation was linked to the total number of particles (N), a hydrodynamic constant ($\mathrm{K_o}$), which depends on the fluid dynamics and determines the probability of collision of suspended crystals, P is the orientation factor, which is related to the orientation of crystals at the moment of collisions, the contact time (τ) of the crystals, the probability of strong (not destroyed at subsequent collisions [W_1]) nucleus bridges between crystals, and the probability of intergrowth of contacting crystal (W).

In lactose refining, formation of aggregated crystals is not desirable. The aggregated crystals cause substantial entrainment of the mother solution, making the subsequent separation (centrifugation) and washing procedure difficult (Shi and others 2006). In the process developed by Shi and others (2006), crystal aggregation was avoided by (1) creating a gradual transition from the initial nuclei formation phase to the rapid growth phase, and (2) cocurrent operation in the crystal rapid growth phase with the flow of the solution and crystals in the same direction. In more conventional stirred crystallization process, aggregation was reduced by (1) increasing the rotational speed of the impeller or lowering the residence time (lower τ in Eq. (5); Wong and others 2010), (2) reducing the amount of seed crystals added at the start of the crystallization process (lower N in Eq. (5); Wong and others 2010), and (3) operating in the upper MSZW region (Wong and others 2012), which will be discussed further in the section on approaches to improve lactose refining.

Industrial Lactose Refining

The three phases in industrial lactose refining are concentration, crystallization, and purification (McSweeney and Fox 2009). A schematic flow chart of the manufacturing process is shown in Figure 6. The evaporation process concentrates the lactose in whey by removing the water. The whey permeate is concentrated to about 65% to 70% total solids (TS) with between 39% and 56% lactose (Table 1). The concentrated whey or permeate is fed to a batch crystallization tank where lactose crystals form during a gradual cooling process. Crude lactose is separated from the mother liquor by centrifugation. Then, the crude lactose is washed and centrifuged again to remove traces of impurities and increase the purity of the final product.

In many dairy plants, the crystallization process is commonly conducted in an agitated jacketed crystallizer. The condensed whey leaves the evaporator at a temperature between 65 °C and 70 °C, and is cooled to between 20 °C and 25 °C to maximize lactose crystal yield (Shi and others 2006). The cooling proceeds over a period of 12 to 48 h (Paterson 2009). As the solution is cooled, the lactose crystals crystallized because of the increase in supersaturation. The yield is commonly calculated as % recovery:

$$\%\ \text{recovery} = \frac{\text{Mass of lactose crystal}\left(\frac{\text{g}}{\text{100g water}}\right)}{\text{Initial mass of lactose in whey concentrate}\left(\frac{\text{g}}{\text{100g water}}\right)} \times 100 \tag{7}$$

Eq. (7) (% recovery) is the common approach used in the industry. However, this approach does not account for the amount of lactose that cannot be crystallized out because of solubility. For example, suppose a lactose refining process starts at 68% TS (75% lactose on dry weight basis, [104 g lactose/100 g water]) and ends

Table 4–Influence of additives on lactose crystal growth(the directions of growth are indicated in Figure 1).

Additives/impurities	Impact	Reference
Whey protein	Retains water of crystallization and creates local lactose superstauration spots that are favorable for nucleation, resulting in the production of small crystals/nuclei and retarding crystal growth.	(Mimouni and others 2005)
Riboflavin	Retards growth in the direction of a-axis, resulting in the formation of trapezoidal plates.Inhibits growth of all crystal faces except the 010 face (riboflavin at 100 ppm).	(Leviton 1943; Kreveld and Michaels 1965; Walstra 2003)
Milk fat	Acts as a hydrophobic barrier and limits the diffusion of hydrophilic molecules and the growth of lactose crystals.	(Kelly 2009)
Mineral salts		
LiCl, $MgSO_4$, Ca lactate, $CaCl_2$	Increase in growth rate, decrease in lactose solubility.	(Bhargava and Jelen 1996)
K_2HPO_4	Decrease in growth rate, increase in lactose solubility.	(Bhargava and Jelen 1996)
Lactose phosphate	Retards growth by adsorbing onto several of the lactose faces, and then it is incorporated.	(Visser and Bennema 1983; Hartel and Shastry 1991; Lifran and others 2007)
Lactic acid	Retards lactose crystallization.	(Jelen and Coulter 1973a)
KCl	Promotes (<5% impurity level) and inhibits growth (>5% impurity level).	(Jelen and Coulter 1973a)
$CaCl_2$	Promotes (<10% impurity level) and inhibits growth (>10% impurity level).	(Jelen and Coulter 1973a; Guu and Zall 1991)
NaH_2PO_4	Promotes growth.	(Jelen and Coulter 1973a; Guu and Zall 1991)
Combination of K^+, Ca^{2+}, PO_4^{3-}	Reduces the relative gross yield of lactose crystallization.	(Guu and Zall 1991)
Interaction of K^+ and PO_4^{3-}	Reduces the relative gross yield of lactose crystallization.	(Guu and Zall 1991)
Structurally related additives (SRA)		
β-lactose	• Influences the type of crystals produced. Inhibits the growth of needle or prism form crystals. • Strong growth inhibitor at low (≈ 20% to 25%) supersaturations. • Influences the morphology of α-lactose crystals. Major growth in • c-direction (low levels (10%) of β-lactose) • a and b directions (high levels (40%) of β-lactose) ∗ (study conducted in DMSO to minimize effect of mutarotation)	(Nickerson and Moore 1974; Raghavan and others 2001; Garnier and others 2002; Dincer and others 1999)
β-cellobiose,α-galactose, Maltitol	Modify crystal habit during crystal growth. Produce flattened crystal with dominant length increase along a direction.	(Garnier and others 2002)
α-glucosamine HCl	Produce elongated crystal with large length increase along b direction.	(Garnier and others 2002)
Sucrose	• Prevent full lactose crystal (Figure 1) development. Produced short and stubby crystals with little development at the base and apex. No effect on the crystal shape of α-lactose crystal (when tested at 10% sucrose w/w).	(Hunziker and Nissen 1927; Garnier and others 2002)
Trisaccharide galactosyl lactose	Prevents normal attachment and orientation of lactose molecules on to the growing crystal, leading to "needle" shape crystals.	(Smart and Smith 1992)
Other compounds		
Gelatine	Reduces crystallization rate by 25% to 60%. However, it does not suppress nucleation in highly supersaturated lactose solutions.	(Ganzle and others 2008)
Alcohols	Reduces the solubility of lactose and supports spontaneous nucleation.	(Ganzle and others 2008)

at 20 °C, where the final solubility is (19.1 g lactose/100 g water; Figure 3). The maximum recovery is 84.9 g lactose/100 g water; however, the % recovery would be calculated as 81.6% Eq. (7), even though all the lactose that could be crystallized at equilibrium would have been collected. To calibrate the yield against the equilibrium value, the efficiency of the crystallization process can be better estimated as the % theoretical yield as defined in Eq. (8).

$$\%\ \text{theoretical yield} = \frac{0.95 \times \text{Mass of lactose crystal obtained}\left(\frac{\text{g}}{\text{100g water}}\right)}{\text{Maximum theoretical crystal yield}\left(\frac{\text{g}}{\text{100g water}}\right)} \times 100 \quad (8)$$

Here the factor, 0.95, accounts for the weight of water in the monohydrate. For the above example, a 100% theoretical yield would be equivalent to 89.4 g α-lactose monohydrate crystal per 100 g water.

Actual plant yields are usually lower than the maximum theoretical yields because of inefficiencies in the postcrystallization procedures (harvesting and washing stages) in the plants (Paterson 2009). A 65% recovery is commonly reported (Paterson 2009). Typical lactose crystals produced through an industrial process are shown in Figure 7 (A). These crystals have wide crystal size distribution (CSD) with huge population of fines (lactose crystal of size < 100 μm). Many of the industrial problems in lactose refining can be traced to the fines, which end up being lost during the recovery/washing operation. They either are lost in the mother liquor (DLP) or are recycled to the evaporators, which increases the water load in the process and hence, larger loss (Paterson 2009). The efficiency of the lactose refining process can be improved by limiting the production of fines (to be discussed in the section on approaches to improve lactose refining).

Apart from cooling crystallization, continuous evaporative crystallizer is starting to gain popularity because of the higher percentage recoveries that can be obtained (Dinesen and Henningfield 2003). Direct application of evaporative crystallization is

complicated by the presence of calcium (complex) salts, such as phosphate and citrate that would results in fouling on the heat exchanger surfaces. Therefore, the whey permeate must be demineralized before or during evaporation using electrodialysis, ion exchange resin, or other calcium chelating agents.

The by-product of lactose refining is de-lactosed permeate (DLP). The composition of DLP varies, depending on the specific processes and their respective efficiencies. The general composition of DLP is summarized in Table 5. Currently, DLP is only being used as animal feed or simply field spread. Some research has been done to explore the use of DLP as a food ingredient. However, the high water content of DLP (60% to 75%) limits direct incorporation into food products. Bund and Hartel (2010) developed a method to dry DLP using proteins (whey proteins isolate, WPI) as codrying agent. DLP with added WPI desorbed to lower water content and picked up less moisture compared to only DLP during moisture desorption and adsorption studies, respectively, suggesting a possibility of obtaining better dried,

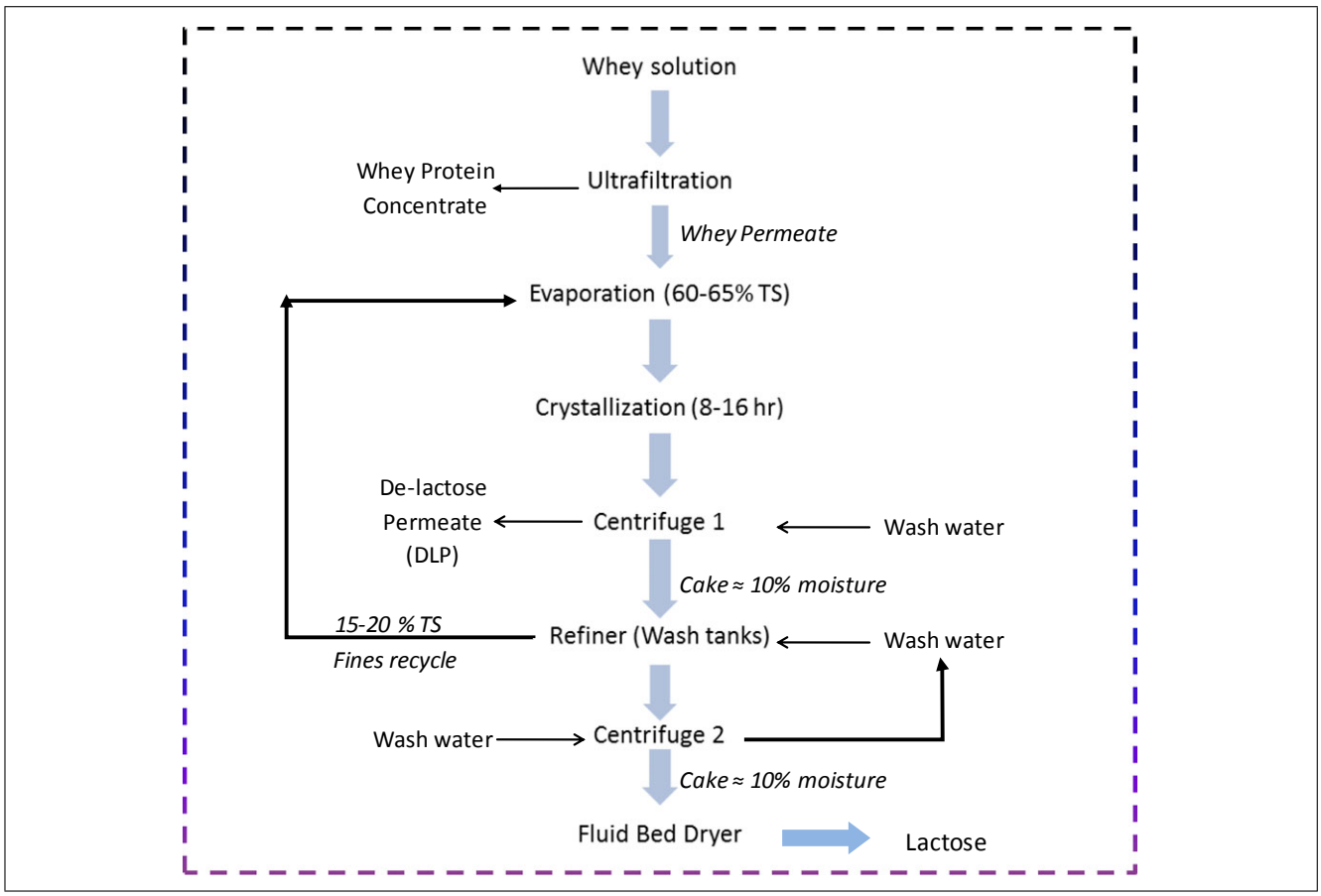

Figure 6–Flow chart of the manufacture of food grade lactose (TS, total solids).

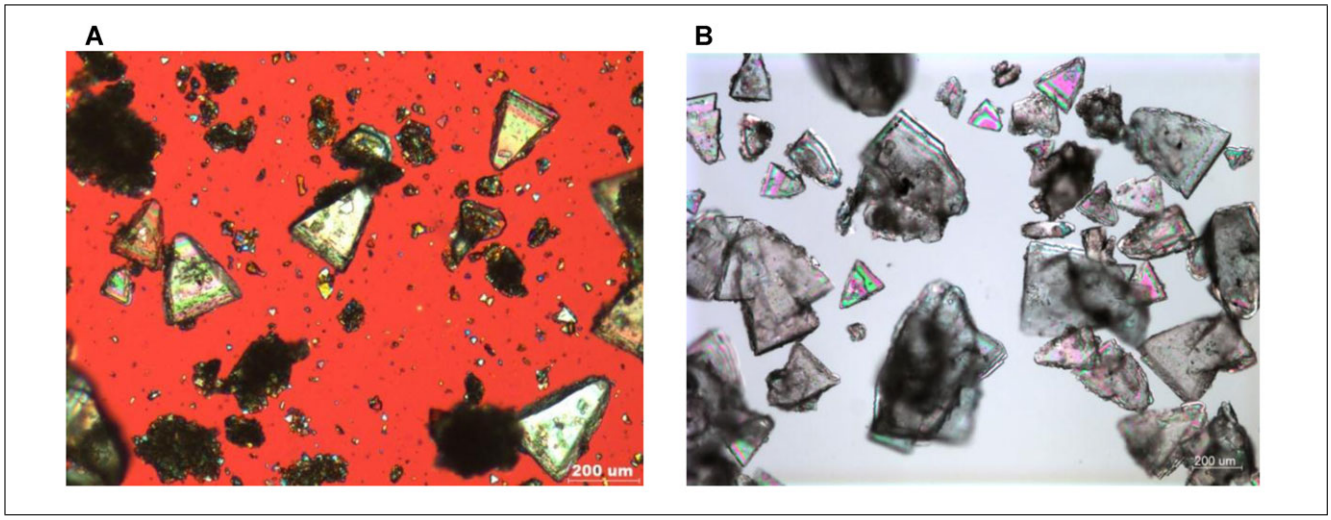

Figure 7–Microscopic image of lactose collected from the crystallizer of (A) a current commercial process (B) an improved crystallization process (Wong and others 2012).

Table 5–Composition of DLP (Liang and others 2009).

	Composition
Moisture (g H_2O/100 g of DLP)	64.4 to 74.1
Constituent (g/100 g of dry matter)	
Sugar profile	
Fructose	<0.4
Galactose	<0.4 to 3.9
Glucose	<0.4 to 1.7
Sucrose	<0.4
Lactose	41.3 to 64.2
Maltose	<0.4
Total Sugars	46.9 to 68.1
Acid profile	
Acetic acid	<0.2
Citric acid	3.5 to 5.7
Lactic acid	2.5 to 7.3
Malic acid	<0.2
Total acids	8.2 to 12.2
Mineral profile	
Calcium	0.7 to 1.1
Magnesium	0.2 to 0.3
Phosphorus	1.6 to 2.3
Potassium	3.9 to 8.4
Sodium	1.2 to 2.3
Chloride	1.3 to 5.5
Total minerals	9.3 to 19.9
Protein content	1.4 to 2.4

stable product. Such products would have potential for use in various food applications like bakery, frozen desserts, confectionery, soups, and sauces.

Modeling the Lactose Crystallization Process

A lactose crystallization process can be modeled via mechanistic models, such as the mass balance equations, whereas the dynamic evolution of the crystal size can be modeled by the population balance model (PBM). Vu and others (2003, 2005, 2006) derived dynamic models of an α-lactose monohydrate crystallization process for cooling batch, cooling and evaporative semi-batch, and cooling in continuous mode crystallization. The dynamic model was a mechanistic model derived from mass and population balances that related the processing parameters to the CSD.

There have been limited reports on the use of PBM to model the lactose crystallization process. For one, PBM was used to analyze the product CSD in a continuous lactose crystallization process (Shi and others 1990) from which crystallization kinetics (nucleation and growth rates) were determined. Vu and others (2006) used PBM as one of the essential components to develop a dynamic model for an α-lactose monohydrate crystallization process. The model was applied to estimate process parameters that produce uniform crystals distribution with the highest yield. In this section, both mechanistic and PBMs will be discussed.

Process dynamics model

For cooling crystallization process, the model proposed by Vu and others (2003, 2005, 2006) excluded nucleation. However, as evidence in Figure 7 (A), secondary nucleation increases the number of crystals in suspension, and thus, should be included in the model. In 2012, the model (Vu and others 2003, 2005, 2006) was refined by Wong and others (2012) to include the change in the number concentration of lactose crystals generated by nucleation.

Assuming that mass transfer by agglomeration or breakage is minimal, the species conservation of water, dissolved impurity, dissolved lactose, and α-lactose crystals for batch crystallization can be written as follows (Wong and others 2012).

Water concentration (x_1; g water/mL solution),

$$\frac{dx_1}{dt} = -0.05\frac{dx_3}{dt} \tag{9}$$

Lactose concentration (x_2; g lactose/mL solution),

$$\frac{dx_2}{dt} = -0.95\frac{dx_3}{dt} \tag{10}$$

Suspension density of crystals (x_3) (g lactose crystal/mL solution),

$$\frac{dx_3}{dt} = \frac{\rho\pi NGx_4^2}{2} \tag{11}$$

Volume equivalent average diameter of crystals (x_4; m),

$$\frac{dx_4}{dt} = G = 3.2\times10^9 e^{\frac{-22}{R(T+273)}}(S-1)^{2.4}/39 \tag{12}$$

Number concentration of crystals, N (#/m^3 solution)

$$\frac{dN}{dt} = B^o = 1.2\times10^{18} e^{\frac{-11.4}{R(T+273)}}(S-1)^{1.5}x_3/258 \tag{13}$$

In this model, the monohydrate crystal (Eq. 11) is produced from 95% dissolved lactose (Eq. 10) and 5% water (Eq. 9). For a seeded batch crystallization process, N (Eq. 11) is the total number density of seed crystals (number/mL solution) introduced at $t = 0$ min. The change in N is triggered mainly by nucleation (Eq. 13) with rate of (B^o; #/mL-min). G (m/min) is the growth rate (Eq. 12). The supersaturation (S) is dependent on the temperature for a cooling crystallization process. S can be calculated by Eq. (1)–(4). The cooling profile required to achieve operation along any regions outlined in the lactose "supersolubility" diagram (Figure 8) can be estimated by solving Eq. (9)–(13) and (1)–(4) with the ordinary differential equation (ODE) solver in Matlab R2008a (Wong and others 2012).

Population balance model

Population balances are widely used to model dynamic particle or droplet size distributions, such as those seen in aggregation, flocculation, crystallization, bubble or droplets in solvent extraction or flocculation columns. Fundamental to the formulation of PBM is the assumption that there exists a number density of particles at every point in the particle state space (Smart and Smith 1992). The population balance is given as (Randolph and Larson 1988):

$$\frac{\partial n}{\partial t} + \nabla\cdot(\vec{v}n) - \text{Birth} + \text{Death} = 0 \tag{14}$$

Here, n is the population density,

$\vec{v}$ is the set of internal and external coordinates, where $\vec{v} = \vec{v}_i + \vec{v}_e$, and

$$\text{Birth} = \text{Birth}_{agg} + \text{Birth}_{br}$$

$$\text{Death} = \text{Death}_{agg} + \text{Death}_{br}$$

Birth and Death represent empirical birth and death density functions at a point in phase space that occur through aggregation (agg) and breakage (br). This equation, coupled with mass, energy and momentum balances, crystallization kinetics and boundary conditions representing the entry and exit of particle suspension, can be used to completely model the formation of the crystals and the dynamics of the crystallization.

The birth and death function for aggregation of 2 particles (volume u and $v - u$) into a single particle volume v can be represented by (Hartel and Randolph 1986):

$$\text{Birth}_{\text{agg}}(v) = \frac{1}{2}\int_0^v K(u, v-u)\, n(u,t)\, n(v-u,t)\, \text{du} \quad (15)$$

$$\text{Death}_{\text{agg}}(v) = n(v,t)\int_0^\infty K(u,v)\, n(u,t)\, \text{du} \quad (16)$$

The aggregation kernel, $K(u,v)$, measures the aggregation frequency between particle (volume u) with another one (volume v; Bramley and others 1996). The aggregation kernel should be selected based on the aggregation mechanism (Hartel and Randolph 1986; Smit and others 1994, Bramley and others 1996). In a length-based form, (Eq. 15 and 16) become (Hounslow and others 1988):

$$\text{Birth}_{\text{agg}}(L) = \frac{L^2}{2}\int_0^L \frac{K\left[\left(L^3-\delta^3\right)^{1/3}, \delta\right] n\left[\left(L^3-\delta^3\right)^{1/3}\right] n(\delta)\, \text{d}\delta}{\left(L^3-\delta^3\right)^{2/3}} \quad (17)$$

$$\text{Death}_{\text{agg}}(L) = n(L)\int_0^\infty K(L,\delta)\, n(\delta)\, \text{d}\delta \quad (18)$$

The birth and death terms because of the breakage mechanisms is (Costa and others 2007),

$$\text{Birth}_{\text{br}}(v) = \int_0^\infty \gamma(u)\, b(u)\, p\left(\frac{v}{u}\right) n(u,t)\, \text{du} \quad (19)$$

$$\text{Death}_{\text{br}}(v) = -b(v)\, n(v,t) \quad (20)$$

where $\gamma(u)$ is the number of daughter particles originated from the breakup of a particle of size u, $b(u)$ is the breakup rate of a particle (size u), and $p(v/u)$ is the fraction of daughter particles with size between v and $v + \text{d}v$.

Solving PBM

PBM can be solved via a stochastic or deterministic framework. The selection is usually based on the importance of the particle population fluctuations (Rawlings and others 1993). Stochastic methods have the advantage of satisfying mass conservation as well as correctly accounting for fluctuations that arise as the system mass accumulates in a small number of large aggregates (Marchisio and others 2003). In lactose crystallization, the CSD data are commonly modeled by deterministic framework. The Method of Moments (MOM) will be reviewed in this section.

In most crystallization systems, some average or total quantities are sufficient to represent the particle distribution. Therefore, the PBM can be transformed into a series of moment equations with regard to the internal coordinate properties (Randolph and Larson 1988). For a crystallization process with the particle size (L) as the only internal coordinate, the PBM (Eq. 14) can be rewritten as,

$$\frac{\text{d}m_i}{\text{d}t} + \nabla\cdot(\vec{v_e} m_i) = 0^i B^o + j G m_{i-1} + \overline{\text{Birth}_i} - \overline{\text{Death}_i} \quad (21)$$

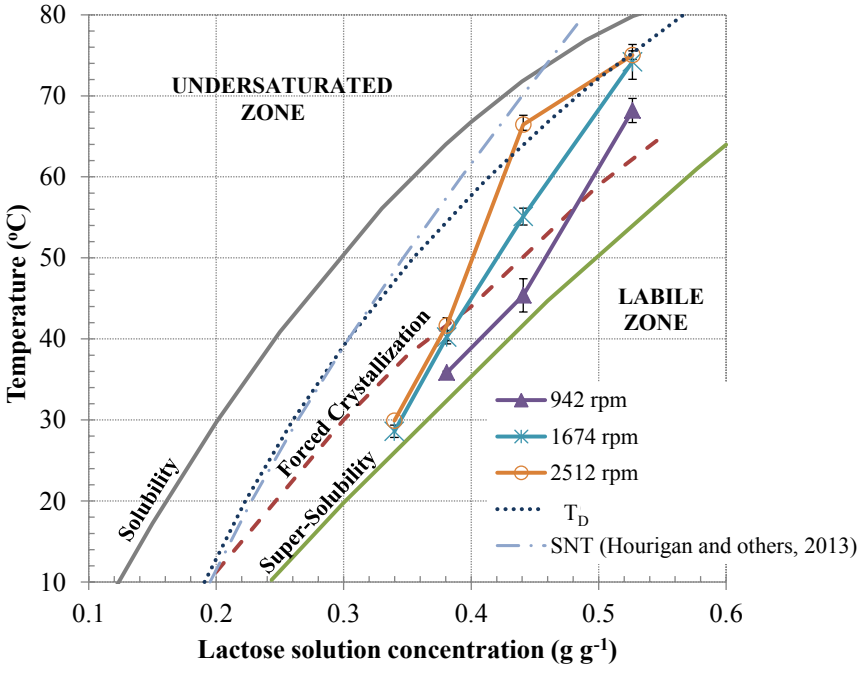

Figure 8–Refined lactose "supersolubility" diagram proposed in 2011.

$$\text{Here}, m_i = \int_0^\infty L^i n(L)\, dL \quad (22)$$

$$\overline{\text{Birth}_i} = \int_0^\infty L^i \text{Birth}(L)\, dL \quad (23)$$

$$\overline{\text{Death}_i} = \int_0^\infty L^i \text{Death}(L)\, dL \quad (24)$$

B^o and G are the nucleation and growth rates.

For size independent aggregation, (Eq. 17 and 18) and (Eq. 23 and Eq. 24) can be reduced to (Hounslow and others 1988):

$$\overline{\text{Birth}_i} = \frac{\beta_o}{2} \int_0^\infty n(\delta) \int_0^L \left(\lambda^3 + \delta^3\right)^{i/3} n(\lambda)\, d\lambda d\delta \quad (25)$$

$$\overline{\text{Death}_i} = \beta_o \int_0^\infty L^i n(L) \int_0^\infty n(\delta)\, d\delta d\, L = \beta_o m_o m_i \quad (26)$$

Here, $\lambda^3 = L^3 - \delta^3$ and β_o is the size-independent aggregation rate.

This simplification greatly reduces the dimension of the internal coordinate of the particle state phase. (Eq. 21) can be solved together with the mass, momentum and energy conservation equations to yield a complete mathematical description of the crystallization process (Randolph and Larson 1988).

For any total number of moments (I), (Eq. 21) forms a closed set in terms of the moments m_i. Therefore, MOM can be easily implemented with an ODE solver. However, it is a challenge to solve the inverse problem. Full reconstruction of the CSD is limited, since the detailed information of the CSD is lost after the transformation (Giaya and Thompson 2004; John and others 2007). The most common approaches have been reviewed by John and others (2007).

Estimating crystallization kinetics using PBM

The power of the PBM in analyzing lactose crystallization is commonly illustrated by its application in mixed suspension mixed product removal (MSMPR) crystallizers (Shi and others 1990; Liang and Hartel 1991; Wong and others 2010). Depending on the assumptions, the PBM was formulated or simplified into forms where crystallization kinetics can be calculated from experimental CSD data.

By assuming (1) steady state, (2) no aggregation or breakage (Birth and Death terms in (10) are equal to zero), (3) size independent growth (McCabes ΔL law, $G \neq G[L]$), (4) near zero-sized nucleation ($B^o = \frac{dN}{dt}\big|_{L\to 0}$), (5) well-stirred (backmixed) reactor, and (6) the feed stream is clear ($n_{in} = 0$), the PBM can be simplified to

$$n = n^o \exp\left(-\frac{L}{G\tau}\right) \quad (27)$$

Here, n is the population density function ($\frac{\#}{\mu m\ mL}$), n^o is the population density of zero-sized nuclei ($\frac{\#}{\mu m\ mL}$), L is the crystal size (μm), G is the linear crystal growth rate (μm/min), and τ is the residence time (min). The nucleation rate is the rate of appearance of zero-sized particles,

$$B^o = n^o G \quad (28)$$

A linear expression between n and L can be established through a semi-logarithmic transformation of the linear PBM (Eq. 28). Crystallization kinetics (G, B^o) may be interpreted from the intercept (ln [n^o]) and the slope ($-\frac{1}{G\tau}$) of the fitted straight line. However, this model (Eq. 28) was shown to be unsatisfactory for lactose crystallization, particularly at small particle sizes (Liang and others 1991). As shown in Figure 9 (A), the linear model only covered part of the experimental CSD data, and the curvature at smaller and larger sizes was ignored. For lactose crystallization, this curvature was because of growth rate dispersion (GRD; Liang and others 1991). GRD is used to describe the growth phenomenon where crystals of the same size grow at different rates because they are subjected to different environments within the crystallizer or because of the inherent structural conditions that differ from crystal to crystal (Randolph and Larson 1988). In this case, assumption (3) for MSMPR operation is no longer valid; that is, $G = f_G(g)$, where $f_G(g)$ is a representation of growth rate distribution models.

When GRD is observed in crystallization, the curvature at small sizes (<50 μm) in the semi-logarithmic plot of n (number density) versus L (particle size) can no longer be accounted for by simple linear extrapolation (Liang and others 1991). Instead, the crystallization kinetics should be calculated by the moment transfer technique, the details of calculation method can be found in Liang and others (1991). The CSD prediction of the GRD models is shown in Figure 9 (B). Compared to the limited range modeled by the linear PBM (Figure 9 A), the GRD model covered the entire range of size distribution. The value of growth and nucleation rates estimated by linear and GRD models are summarized in Table 6. Clearly, the linear model discounted the nucleation rate and overestimates the average growth rate.

As discussed earlier, crystal aggregation might occur during lactose refining. When aggregation occurs in a MSMPR operation, assumption (2) is no longer valid, and should be replaced by alternative terms that describe the aggregation process. To account for aggregation in an MSMPR lactose crystallization process, Wong and others (2010) included size independent aggregation functions (Eq. 25 and 26) in the PBM. In contrast to the linear and GRD models, Wong and others (2010) solved the PBM using particle volume as the internal coordinate. Therefore, the crystallization kinetics (G_v, B^o, β_o) shown in Table 6 are volume-based kinetics. The kinetic rates of crystallization depend largely on the solution approach to PBM. For lactose crystallization, the linear PBM and GRD approaches have been most commonly used. However, when a large amount of aggregation/breakage is observed, care should be taken to avoid oversimplifying the PBM.

Empirical kinetic expressions can be obtained by conducting the MSMPR experimental procedure for a variety of processing conditions (for example, temperatures, agitation rate, supersaturations, and so on). The secondary nucleation rate (B^o) is often correlated to operating conditions through Arrhenius or power law expressions. Eq. (29)–(31) are examples of such models proposed respectively by Liang and others (1991), Rawlings and others (1993), and Davey and Garside (2000).

$$B^o = k_{oN} \exp\left(-\frac{E_{aN}}{R\, T_k}\right) (S-1)^n\, M_T^j \quad (29)$$

Table 6–Crystallization kinetics calculated from 3 methods.

	Growth rate (G)	Nucleation rate (B^o, #/mL min)	Aggregation rate (β_o)
Linear PBM (Shi and others 1990)	0.77 μm/min	3.27E + 03	–
Moment transfer technique (Liang and others 1991)	0.26 μm/min	3.35E + 04	–
Moment transformation method (Wong and others 2010)	38.1 $(\mu m)^3$/min	18E + 6	1.34E-12 (m^3/#-s)

$$B^o = k_b \exp\left(-\frac{E_{a\,N}}{\mathrm{R}\,T_k}\right)(S)^n\, m_i^j \tag{30}$$

$$B^o = k_b\,(\mathrm{rpm})^k\,(\Delta c)^n\, M_T^j \tag{31}$$

Here, k_b, n, j, k, k_{oN} are considered to be empirical constants, m_i is the i^{th} moment of the CSD, S and Δc are the supersaturation, M_T is the suspension density, E_{aN} is the activation energy for nucleation, and T_k is the temperature in Kelvin (K). These parameters (k_b, n, j, k, k_{oN}, E_{aN}) can be regressed from sets of experimental crystallization rate data.

For nucleation rate, empirical power law models comprises of supersaturation (S) and suspension density (M_T, m_3) are commonly found. Most models predict j close to one, suggesting the dominance of crystals–vessel walls collisions, or, crystal–stirrer rather than crystal–crystal collisions (Garnier and others 2002). Eq. (29) and (30) are based on the standard Arrhenius kinetics model, where the contribution of agitation was not considered. However, the effect of agitation is especially important in contact nucleation, where the values of k (Eq. 31) predicted are in the range of 2 to 4 (Davey and Garside 2000).

The growth rate is correlated in a similar way. Eq. (32) is commonly suggested to represent growth of crystals (Liang and others 1991; Rawlings and others 1993; Arellano and others 2004):

$$G = k_{o\,G} \exp\left(-\frac{E_{a\,G}}{\mathrm{R}\,T_k}\right)(S-1)^m \tag{32}$$

where k_{oG} and m are empirical constants and E_{aG} is the activation energy for crystal growth. The parameters (k_{oG}, m and E_{aG}) are regressed from sets of experimental crystallization rate data. In (Eq. 32), the temperature dependence was incorporated by an Arrhenius-type expression (Rawlings and others 1993). The value of m is commonly reported in the range of 2 to 3, where a value of m greater than 2 might indicate the effects of the β-lactose impurity on crystal growth (Shi and others 1990). In the literature, the value of E_{aG} was between 22 to 24 kcal/mol. The high E_{aG} indicated that the growth of lactose crystals is most likely a surface integration mechanism, where the growth rate is determined by the rate that lactose molecules were incorporated into the crystal lattice (Shi and others 1990).

For lactose crystallization, similar expressions for aggregation is lacking. To overcome the complex relationship of aggregation rate and processing parameters, a kinetic model was developed based on artificial neural network (ANN; Wong and others 2010). For an MSMPR crystallizer, the ANN model predicted higher aggregation rate with high amount of seed crystals and low residence time. On the contrary, aggregation reduces at high agitation speed and supersaturation had minimal impact (Wong and others 2010).

Approaches to Improve Lactose Refining

To overcome the industrial problem of the over-production of fines, the ideal operating conditions should be predicted through careful examination of the fundamentals of lactose crystallization process. The following approaches have been suggested for improving lactose refining.

Cooling profile

In the lactose "supersolubility" diagram, the conditions at which different crystallization phenomena occurs during the crystallization process are defined, as shown in Figure 8. The significant

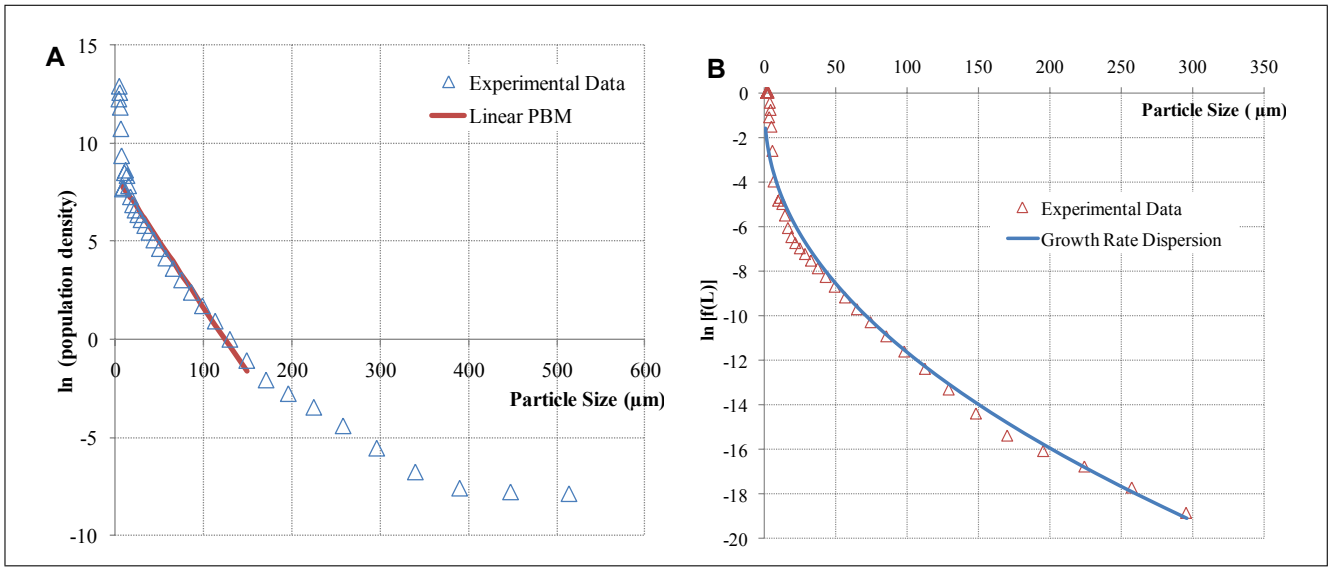

Figure 9–Typical Crystal Size Distribution (CSD) obtained from a continuous MSMPR experiment presented as (A) Semilogarithmic plot of population density versus crystal size (B) Normalized population densities calculated for gamma distributions using the moment transfer technique (Liang and others 1991).

concepts presented in Figure 8 are summarized as (Hunziker 1926; Nickerson and Moore 1974; Wong and others 2011):

(1) In the unsaturated zone, growth and nucleation cannot occur.
(2) In the metastable and labile zones, crystal growth can occurs.
(3) In the labile zone, spontaneous nucleation can occurs without the presence of seeds.
(4) In the metastable zone, crystallization can only occurs after crystal seeds addition. The crystals seeds can be lactose, substances containing lactose, or substances that are isomorphous to lactose.
(5) When the crystallization process is seeded, the metastable zone can be split into the upper and lower zones by the forced crystallization line.
   - In the upper region (between the solubility and the forced crystallization lines; Figure 8), crystallization is dominated by crystal growth, and the secondary nucleation is suppressed.
   - In the lower region (between the forced crystallization and the supersolubility lines; Figure 8), secondary nucleation dominates, especially when the process is seeded at conditions close to the forced crystallization line.

Therefore, the upper mestastable region is ideal for an industrial crystallization process where crystal growth should dominate. However, the MSZW depicted by the forced crystallization line in Figure 8 was developed for the mass crystallization of sweetened condensed milk. Therefore, it is not suitable for a commercial lactose crystallization process.

The dynamic metastable limit (for an industrial lactose crystallization process) was refined by Wong and others (2011), as shown in Figure 8. The first detection (T_D) curve indicates the first generation of nuclei as cooling progresses at each supersaturation. At concentrations below 0.35 g anhydrous lactose/g solution, the T_D line overlaps with the secondary nucleation threshold (SNT, $C_{SNT} = e^{2.992+0.196T}$ [g anhydrous lactose/100g water]) proposed by (Butler and others 1997). Therefore, the equivalent upper metastable region is the region between the final solubility and the T_D line (Region 1, that is, operating region with enhanced growth and minimum secondary nucleation). The T_D line is independent of agitation speed (Wong and others 2011). The other 3 reference lines for different agitation speeds (942, 1674, and 2512 rpm) indicate the temperatures where transmittance changed (ΔT_r; via spectroscopy test) because of secondary nuclei formation by 1% at different agitation speed. The upper MSZW defined by the region between solubility and the 1% ΔT_r lines have medium level of secondary nucleation.

The information displayed in Figure 8 is extremely useful when designing the processing parameters (for example, cooling profile, agitation rate). To produce large particles with minimum fines (<100 μm), crystal growth should be minimize, whereas suppressing secondary nucleation. Thus, the upper metastable region (Region 1) is a good candidate, as shown in Figure 8. However, region 1 might not be ideal in term of operation (slow cooling, long operation time). Depending on the acceptable operational cost and extent of secondary nucleation, the crystallization process can be tune accordingly. In this case, the region between $T_{\text{solubility}}$ and one of the 3 reference lines (942, 1674, and 2512 rpm) might be acceptable (Figure 8). In addition, the upper MSZW decreases with higher degree of agitation (Figure 8). Therefore, it is necessary to maintain adequate stirring for heat transfer and uniformity, but minimum stirring to avoid secondary nucleation. This principle will be developed further in the context of industrial cooling profiles in the next section.

Whey pretreatment before crystallization process

Lactose is produced from whey permeate, which contains lactose, minerals, riboflavin, and traces of fat and protein (Table 1). The impact of these components on the crystallization rate has been reported frequently (Jelen and Coulter 1973a; Guu and Zall 1991; Mimouni and others 2005; Gernigon and others 2010), as shown in Table 2 and 3. To improve the separation efficiency and the yield (recovery), whey solution can be pretreated before the crystallization operation.

During lactose refining, the impact of protein on lactose crystallization process is minimized because the whey protein has been removed via ultrafiltration. Therefore, protein should have little effect on lactose crystallization from whey permeate. The impact of riboflavin on crystallization rate is minimal (Smart and Smith 1992) and thus, it is not removed before crystallization. After crystallization, the riboflavin adsorbed onto lactose crystals (yellow color) is washed off in the subsequent washing/ refining steps (Figure 6).

An important factor controlling yield and purity in lactose crystallization is the mineral content of the whey permeate (Hoppe and Higgins 1992). As shown in Table 4, most minerals affect crystal growth and thus, the yield of lactose. The effect of minerals can be reduced by demineralization of whey permeate, which increases the purity (Mikkonen and others 2001) and the yield of lactose (Harper 1992). Nanofiltration (NF) is a potential process for partial demineralization of whey permeate (Cuartas-Uribe and others 2010). This process reduces more than 50% of the nutritionally unfavorable minerals (especially monovalent cations, for example, Na and K), whereas retaining some nutritionally favorable minerals (for example, Ca) (Mikkonen and others 2001). The NF retentate (demineralized whey permeate) can be further processed into lactose via the normal crystallization process, as depicted in Figure 6. The NF process increases the yield of lactose by about 6% to 10% (Guu and Zall 1992; Mikkonen and others 2001). In addition, the TS content (especially salt level) of the mother liquor (DLP) decreases, making it possible to be utilized in other commercial products, such as fermentation feedstock (Yang and Silva 1995) rather than animal feed (Mikkonen and others 2001) .

Alternative production pathways

As discussed earlier, cooling crystallization is the most common mode of operation for lactose removal from whey permeate. This mode of operation is based on the principle of reduced solubility and increased supersaturation as the solution cools.

Apart from cooling crystallization, alternative pathways for lactose recovery have also been reported in the literature. For example, lactose was crystallized from "anti-solvent" crystallization through the addition of alcohols in (Bund and Pandit 2007). Alcohol greatly reduces the solubility of lactose (Majd and Nickerson 1976) with longer chain alcohols having lower lactose solubility. Thus, addition of alcohol accelerates crystallization by increasing supersaturation, resulting in precipitation of lactose. Compared to the maximum % recovery (<85%; Eq. (7)) commonly observed in cooling crystallization process, lactose recovery of 85% to 93% was reported at effective ethanol concentration of 65 to 85% (v/v) in a paneer whey system (Bund and Pandit 2007). However, this rapid crystallization process produces small lactose crystals mostly in the range of 3 to 10 μm, which are not typical in the conventional (dairy) industrial lactose refining process.

In the pharmaceutical industry, antisolvent crystallization is frequently used to produce engineered lactose as the excipient for DPI. For DPI, lactose particles that exhibited less elongated and more irregular shape, rougher surface texture, higher surface area are generally preferred (Kaialy and Nokhodchi 2012). These crystals can be produced by controlled antisolvent crystallization where the crystal habit of lactose was customized through the antisolvent addition rate, supersaturation level, and sonication (Kougoulos and others 2010; Kaialy and Nokhodchi 2012).

Technology Transfer: Academic to Industry

All essential components to industrial optimization are presented in earlier sections of this review. This information (and how to use it) might appear obvious for many academics; however, there is still a barrier for the manufacturers to utilize them. This section expands upon the earlier section to illustrate the approach to adapt the new academic findings in the dairy industries. It is generally known that lactose crystallization in the dairy industry is well established and lactose refiners are resistant to change. Any "hard" modification that would require high initial capital investment or excessive modification to current production pipeline will not be readily acceptable. For example, the patented process invented by Shi and others (2006) has shown success in producing large, uniform lactose crystals having narrow CSD; however, the technology has not been adapted widely by the industry because the process involves the use of a nucleator, which is an additional unit operation not currently found in lactose production facilities. Therefore, a "soft" solution (processing parameters optimization only), as outlined earlier, is the best solution.

Industrial crystallizers are commonly constructed with closed clearance impellers operating at low rotational speed (Wong and others 2012). When examining the lactose "supersolubility" diagram (Figure 8) for crystallization at low rpm, additional lines indicating low (T_D), medium-low (0.5% ΔT_r), and medium-high (1% ΔT_r) level of secondary nucleation are indicated in Figure 10 (B). By using Eq. (9)–(13), the lactose concentration profile of a crystallization process with a given cooling profile can be calculated, as illustrated in Figure 10. Through our industrial collaborators, the 22 and 25 h cooling profiles were conducted in a 7000 gal crystallizer (same as that described in Wong and others 2012). The size distributions of the lactose crystals are shown in Figure 11, which show significant improvement in fines reduction over the typical industrial process with 14 h cooling profile. Thus, a well-designed cooling profile, where large crystals can be produced, is essential.

For a lactose crystallization process, an optimized cooling profile is one that produces large crystals (high growth rate) with minimum fines (low secondary nucleation rate) in the shortest possible time. As shown in Figure 12, when choosing a region of operation along the MSZW, an optimal profile should move in the forward direction (from supersolubility to solubility line) to minimize secondary nucleation, but backward direction to maximize growth and to shorten cooling time. Therefore, the challenge is to establish the optimal balance of secondary nucleation, growth, and cooling time.

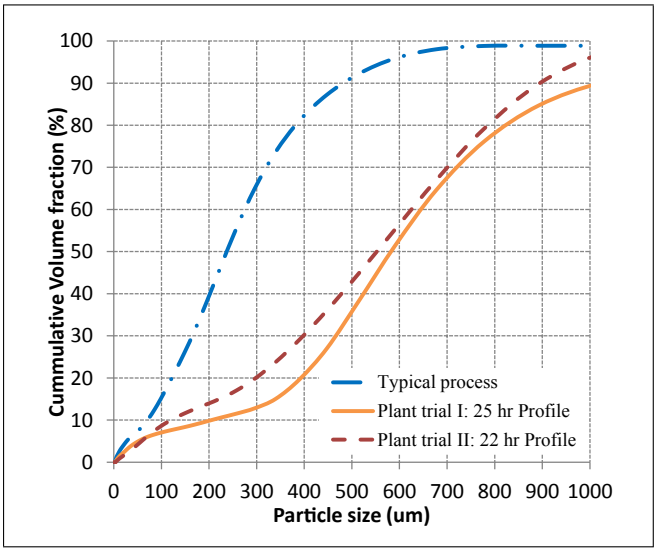

Figure 11–Cumulative crystal size distribution (CSD) from Plant Trials.

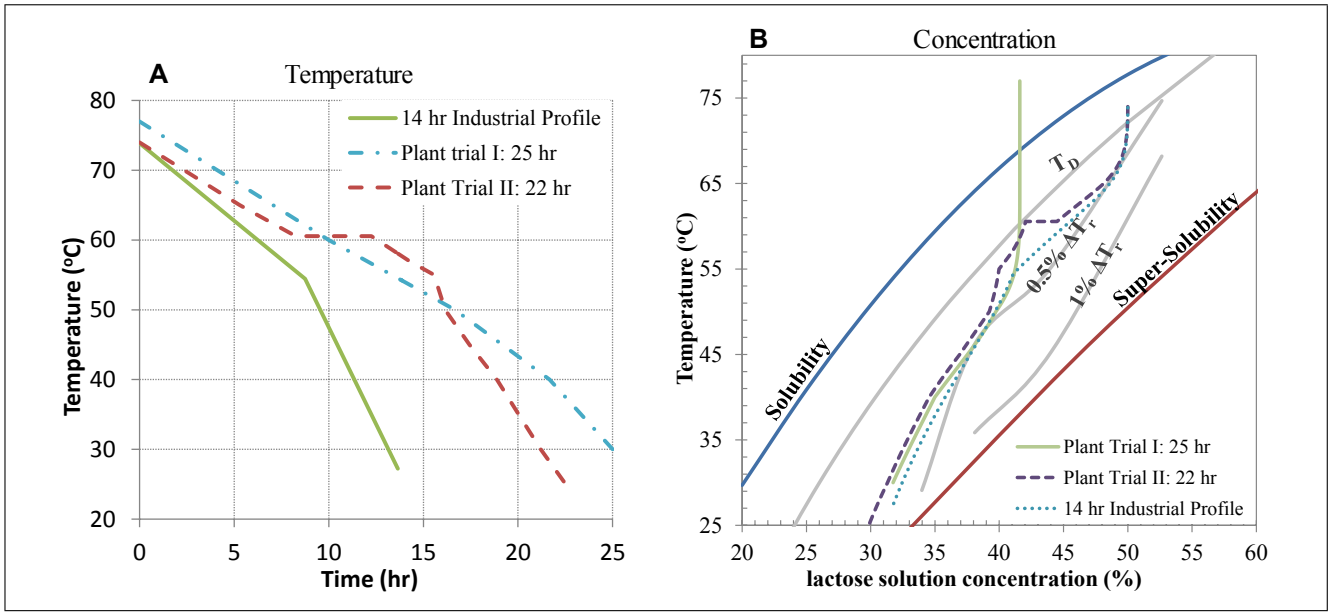

Figure 10–Three (A) cooling profiles, and (B) the corresponding concentration profiles calculated by Eq. (9)–(13).

All plant trials conducted (Figure 10) focused on crystallization operations in regions that were slightly above or close to the 0.5% ΔTr line. Among all the cooling profiles tested for the industrial crystallizer, the 14 h Industrial Profile was the worst in that it produced ≈ 15% fines (Figure 11). In addition, the concentration profile for 14 h Industrial Profile crossed below the 0.5% ΔTr line for concentrations between 46% to 50% and 37% to 40% (Figure 10 B), whereas the profiles for plant trials I & II remained above the 0.5% ΔTr line throughout the crystallization process (Figure 10 B). Based on the concentration profiles, it is likely that the cross-over contributed to the increased extent of secondary nucleation and thus, higher amount of fines produced in the 14 h Industrial Profile.

Based on the concept of maximizing growth and minimizing secondary nucleation, a 13 h cooling profile (Wong and others 2012) was developed with a +1 °C to 2 °C cushion above the 0.5% ΔTr line (Figure 10B). This 13 h cooling profile was successfully implemented on an industrial crystallization process, leading to 28% reduction in fines (crystals < 100 μm). In addition, the new crystals (13 h cooling) had an L_{50} ≈ 360 μm, compared to ≈ 250 μm obtained from the typical process (14 h cooling).

Designing industrial lactose crystallization process is not an art. With the availability of the process model (Eq. (9)–(13) and the refined lactose "supersolubility" diagram (Figure 12), a unique cooling profile can be customized according to the initial concentration of the whey permeate concentrate, the desired cooling time, and the tolerance of fines.

Conclusions

Since the first isolation of lactose in 1633, many researchers have studied and contributed to the understanding of the lactose crystallization process. The fundamental knowledge, including the mechanism of the production of lactose crystals, the principle of crystallizer operation, modeling approaches, and the effects of whey components on the crystallization rate are the keys to designing/optimizing industrial lactose crystallization. For example, the production of fines (particles < 100 μm) can be avoided by maintaining the crystallization operation in the upper metastable zone and the yield of the crystallization process can be improved by removal of whey components that retard crystallization. Much research has been done on various aspects of lactose crystallization; future effort should focus on transferring the technology to the dairy industry.

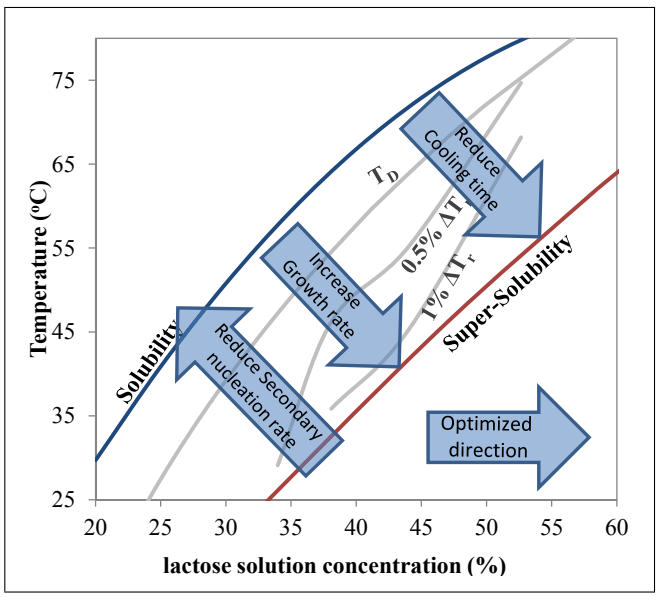

Figure 12–Selecting the directions for optimization according to the lactose "supersolubility" diagram (arrows point in increased direction).

References

Arellano MP, Aguilera JM, Bouchon P. 2004. Development of a digital video-microscopy technique to study lactose crystallisation kinetics in situ. Carbohydr Res 339(16):2721–30.

Bhargava A, Jelen P. 1996. Lactose solubility and crystal growth as affected by mineral impurities. J Food Sci 61(1):180–4.

Booij CJ. 1985. Use of lactose in the pharmaceutical and chemical industry. Int Dairy J 38(4):105–9.

Boutin R. 2005. Lactose: the forgotten sugar. Kennedy's Confection (December):46–7.

Bramley AS, Hounslow MJ, Ryall RL. 1996. Aggregation during precipitation from solution: a method for extracting rates from experimental data. J Colloid Interface Sci 183(1):155–65.

Bund RK, Pandit AB. 2007. Rapid lactose recovery from buffalo whey by use of 'anti-solvent, ethanol'. J Food Eng 82(3):333–41.

Bund RK, Hartel RW. 2010. Effect of protein on sorption characteristics of delactosed permeate. J Food Eng 96(3):388–93.

Butler BK, Zhang H, Johns MR, Mackintosh DL, White ET. 1997. The influence of growth rate dispersion in crystallisation. Proceedings of CHEMECA 97, 25th Australian and New Zealand Chemical Engineer ' s Conference and Exhibition September 29—October 1; Rotorua, New Zealand.

Clydesdale G, Roberts KJ, Docherty R. 1994. Modelling the morphology of molecular crystals in the presence of disruptive tailor-made additives. J Cryst Growth 135(1–2):331–40.

Costa CBB, Maciel MRW, Filho RM. 2007. Considerations on the crystallization modeling: population balance solution. Comput Chem Eng 31(3):206–18.

Cuartas-Uribe B, Vincent-Vela MC, Alvarez-Blanco S, Alcaina-Miranda MI, Soriano-Costa E. 2010. Application of nanofiltration models for the prediction of lactose retention using three modes of operation. J Food Eng 99(3):373–6.

Davey R, Garside J. 2000. From molecules to crystallizers. Oxford: Oxford Univ. Press.

Dincer TD, Parkinson GM, Rohl AL, Ogden MI. 1999. Crystallisation of α-lactose monohydrate from dimethyl sulfoxide (DMSO) solutions: influence of β-lactose. J Cryst Growth 205(3):368–74.

Dinesen R, Henningfield T, inventors; 2003 Oct 23. Process and plant for evaporative concentration and crystallization of a viscous lactose-containing aqueous liquid. U.S. patent US20030196957 A1.

Ganzle MG, Haase G, Jelen P. 2008. Lactose: crystallization, hydrolysis and value-added derivatives. Int Dairy J 18(7):685–94.

Garnier S, Petit S, Coquerel G. 2002. Influence of supersaturation and structurally related additives on the crystal growth of α-lactose monohydrate. J Cryst Growth 234(1):207–19.

Gernigon G, Schuck P, Jeantet R. 2010. Processing of Mozzarella cheese wheys and stretchwaters: a preliminary review. Dairy Sci Technol 90(1):27–46.

Giaya A, Thompson RW. 2004. Recovering the crystal size distribution from the moment equations. AIChE J 50(4):879–82.

Griffiths RC, Paramo G, Merson RL. 1982. Preliminary investigation of lactose crystallization using the population balance technique. AIChE Symp Ser 78118–28.

Guu MYK, Zall RR. 1991. Lactose crystallization : effects of minerals and seeding. Process Biochem 26(3):167–72.

Guu YK, Zall RR. 1992. Nanofiltration concentration effect on the efficacy of lactose crystallization. J Food Sci 57(3):735–9.

Harper WJ. 1992. Lactose and lactose derivatives. In: J. G. Zadow, editor. Whey and lactose processing. New York: Elsevier applied science. p 317–60.

Hartel RW, Randolph AD. 1986. Mechanisms and kinetic modeling of calcium oxalate crystal aggregation in a urinelike liquor. Part II: kinetic modeling. AIChE J 32(7):1186–95.

Hartel RW, Shastry AV. 1991. Sugar crystallization in food products. Crit Rev Food Sci Nutr 30(1):49–112.

Herrington BL. 1934a. Some physico-chemical properties of lactose: I. The spontaneous crystallization of supersaturated solutions of lactose. J Dairy Sci 17(7):501–18.

Herrington BL. 1934b. Some physico-chemical properties of lactose: II. Factors influencing the crystalline habit of lactose. J Dairy Sci 17(8):533–42.

Hobman PG. 1984. Review of processes and products for utilization of lactose in deproteinated milk serum. J Dairy Sci 67(11):2630–53.

Holsinger VH. 1988. Lactose. In: Wong NP, editor. Fundamentals of dairy chemistry. 3rd ed. New York: Van Nostrand Reinhold Co. p 279–342.

Hoppe GK, Higgins JJ. 1992. Demineralization. In: Zadow JG, editor. Whey and lactose processing. New York: Elsevier applied science. p 91–131.

Hounslow MJ, Ryall RL, Marshall VR. 1988. A discretized population balance for nucleation, growth, and aggregation. AIChE J 34(11):1821–32.

Hunziker OF. 1926. Condensed milk and milk powder. 4th ed. La Grange, Illinois: Otto F. Hunziker.

Hunziker OF, Nissen BH. 1926. Lactose solubility and lactose crystal formation: I. Lactose solubility. J Dairy Sci 9(6):517–37.

Hunziker OF, Nissen BH. 1927. Lactose solubility and lactose crystal formation: II. Lactose crystal formation. J Dairy Sci 10(2):139–54.

Jelen P, Coulter ST. 1973a. Effects of certain salts and other whey substances on the growth of lactose crystals. J Food Sci 38(7):1186–9.

Jelen P, Coulter ST. 1973b. Effects of supersaturation and temperature on the growth of lactose crystals. J Food Sci 38(7):1182–5.

John V, Angelov I, Öncül AA, Thévenin D. 2007. Techniques for the reconstruction of a distribution from a finite number of its moments. Chem Eng Sci 62(11):2890–904.

Jones AG. 2002. Crystallization process systems. Oxford: Butterworth-Heinemann.

Kaialy W, Nokhodchi A. 2012. Antisolvent crystallisation is a potential technique to prepare engineered lactose with promising aerosolisation properties: effect of saturation degree. Int J Pharm 437(1–2):57–69.

Kelly PM. 2009. Significance of lactose in milk powders. In: McSweeney PLH, editor. Advanced dairy chemistry volume 3: lactose, water, salts and minor constituents. 3rd ed. New York: Springer. p 80–95.
Kirk JH, Dann SE, Blatchford CG. 2007. Lactose: a definitive guide to polymorph determination. Int J Pharm 334(1–2):103–14.
Kougoulos E, Marziano I, Miller PR. 2010. Lactose particle engineering: influence of ultrasound and anti-solvent on crystal habit and particle size. J Cryst Growth 312(23):3509–20.
Kreveld AV, Michaels AS. 1965. Measurement of crystal growth of α-lactose. J Dairy Sci 48(3):259–65.
Leviton A. 1943. Adsorption of riboflavin by lactose. Ind Eng Chem 35(5):589–93.
Liang B, Hartel RW. 1991. Techniques for developing nucleation and growth-kinetics from MSMPR data for sucrose crystallization in the presence of growth-rate dispersion. J Cryst Growth 108(1–2):129–42.
Liang B, Shi Y, Hartel RW. 1991. Growth-rate dispersion effects on lactose crystal size distributions from a continuous cooling crystallizer. J Food Sci 56(3):848–54.
Liang B, Bund RK, Hartel RW. 2009. Effect of composition on moisture sorption of delactosed permeate. Int Dairy J 19(10):630–6.
Lifran EV, Vu TTL, Durham RJ, Hourigan JA, Sleigh RW. 2007. Crystallisation kinetics of lactose in the presence of lactose phosphate. Powder Technol 179(1–2):43–54.
Linnikov OD. 2008. Mechanism of aggregation and intergrowth of crystals during bulk crystallization from solutions. Cryst Res Technol 43(12):1268–77.
Listiohadi YD, Hourigan JA, Sleigh RW, Steele RJ. 2005. Properties of lactose and its caking behaviour. Aust J Dairy Technol 60(1):33–52.
Lowe EK, Paterson AHJ. 1998. A mathematical model for lactose dissolution, part II. Dissolution below the alpha lactose solubility limit. J Food Eng 38(1):15–25.
Majd F, Nickerson TA. 1976. Effect of alcohols on lactose solubility. J Dairy Sci 59(6):1025–32.
Marchisio DL, Pikturna JT, Fox RO, Vigil RD, Barresi AA. 2003. Quadrature method of moments for population-balance equations. AIChE J 49(5):1266–76.
Mcleod J. 2007. Nucleation and growth of alpha lactose monohydrate. [dissertation]. New Zealand: Massey Univ.
McLeod JS, Paterson AHJ, Bronlund JE, Jones JR. 2010. Nucleation of alpha lactose monohydrate induced using flow through a venturi orifice. J Cryst Growth 312(6):800–7.
McSweeney PLH, Fox PF. 2009. Advanced dairy chemistry. Volume 3. Lactose, water, salts and vitamins. New York, USA: Springer Science+Business Media, LLC. 759 p.
Mikkonen H, Helakorpi P, Myllykoski L, Keiski RL. 2001. Effect of nanofiltration on lactose crystallisation. Milchwissenschaft 56(6):307–10.
Mimouni A, Schuck P, Bouhallab S. 2005. Kinetics of lactose crystallization and crystal size as monitored by refractometry and laser light scattering: effect of proteins. Lait 85(4–5):253–60.
Modler HW, Lefkovitch LP. 1986. Influence of pH, casein, and whey protein denaturation on the composition, crystal size, and yield of lactose from condensed whey. J Dairy Sci 69(3):684–97.
Nickerson TA. 1974. Lactose. In: Webb BH, editor. Fundamentals of dairy chemistry. 2nd ed. Westport, Conn.,: The Avi Publishing Company, Inc. p 273–324.
Nickerson TA, Moore EE. 1974. Alpha lactose and crystallization rate. J Dairy Sci 57(2):160–4.
Paterson AHJ. 2009. Production and uses of lactose. In: McSweeney PLH, editor. Advanced dairy chemistry volume 3: lactose, water, salts and minor constituents. 3rd ed. New York, USA: Springer Science+Business Media, LLC. p 105–20.
Raghavan SL, Ristic RI, Sheen DB, Sherwood JN. 2001. The bulk crystallization of alpha-lactose monohydrate from aqueous solution. J Pharm Sci 90(7):823–32.
Randolph AD, Larson MA. 1988. Theory of particulate processes: analysis and techniques of continuous crystallization. 2nd ed. San Diego: Academic Press Inc.
Rawlings JB, Miller SM, Witkowski WR. 1993. Model identification and control of solution crystallization processes—a review. Ind Eng Chem Res 32(7):1275–96.
Roos YH. 2009. Solid and Liquid States of Lactose. In: McSweeney PLH, editor. Advanced dairy chemistry volume 3: lactose, water, salts and minor constituents. 3rd ed. New York: Springer. p 17–30.
Shi Y, Hartel RW, Liang B. 1989. Formation and growth phenomena of lactose nuclei under contact nucleation conditions. J Dairy Sci 72(11):2906–15.
Shi Y, Liang B, Hartel RW. 1990. Crystallization kinetics of alpha-lactose monohydrate in a continuous cooling crystallizer. J Food Sci 55(3):817–20.
Shi Y, Liang B, Hartel RW, inventors; 2006 Jun 15. Crystal refining technologies by controlled crystallization. U.S. patent US 2006/0128953 A1.
Smart JB, Smith JM. 1992. Effect of selected compounds on the rate of α-lactose monohydrate crystallization, crystal yield and quality. Int Dairy J 2(1):41–53.
Smit DJ, Hounslow MJ, Paterson WR. 1994. Aggregation and gelation—I. Analytical solutions for CST and batch operation. Chem Eng Sci 49(7):1025–35.
Thurlby JA. 1976. Crystallization kinetics of alpha-lactose. J Food Sci 41(1):38–42.
Valle-Vega P, Nickerson TA, Moore EE, Gonzenbach M. 1977. Variability of growth of lactose crystals under commercial treatment. J Dairy Sci 60(10):1544–9.
Visser RA. 1982. Supersaturation of alpha-lactose in aqueous-solutions in mutarotation equilibrium. Neth Milk Dairy J 36(2):89–101.
Visser RA, Bennema P. 1983. Interpretation of the morphology of alpha-lactose hydrate. Neth Milk Dairy J 37(3):109–37.
Vu TTL, Hourigan JA, Sleigh RW, Ang MH, Tade MO. 2003. Metastable control of cooling crystallization. Eur Symp Comput Aided Process Eng 13527–32.
Vu LTT, Durham RJ, Hourigan JA, Sleigh RW. 2005. Dynamic modelling and simulation of lactose cooling crystallisation: from batch and semi-batch to continuous operations. Comput Aided Chem Eng 20:493–8.
Vu TTL, Durham RJ, Hourigan JA, Sleigh RW. 2006. Dynamic modelling optimisation and control of lactose crystallisations: comparison of process alternatives. Sep Purif Technol 48(2):159–66.
Walstra P. 2003. Physical chemistry of foods. New York: Marcel Dekker.
Whittier EO. 1944. Lactose and its utilization: a review. J Dairy Sci 27(7):505–37.
Wong SY, Bund RK, Connelly RK, Hartel RW. 2010. Modeling the crystallization kinetics of lactose via artificial neural network. Cryst Growth Des 10(6):2620–2628.
Wong SY, Bund RK, Connelly RK, Hartel RW. 2011. Determination of the dynamic metastable limit for α-lactose monohydrate crystallization. Int Dairy J 21(11):839–47.
Wong SY, Bund RK, Connelly RK, Hartel RW. 2012. Designing a lactose crystallization process based on dynamic metastable limit. Cryst Growth Des 111(4):642–54.
Wood-Kaczmar M, inventor; 2006 Aug 17. Process for crystallizing lactose particles for use in pharmaceutical formulations. U.S. patent WO 2006/086130 A2.
Yang ST, Silva EM. 1995. Novel products and new technologies for use of a familiar carbohydrate, milk lactose. J Dairy Sci 78(11):2541–62.
Zeng XM, Martin GP, Marriott C, Pritchard J. 2000. The influence of crystallization conditions on the morphology of lactose intended for use as a carrier for dry powder aerosols. J Pharm Pharmacol 52(6):633–43.